32. Holman BL, Hellman RS, Goldsmith SJ, et al. Biodistribution, dosimetry, and clinical evaluation of technetium-99m-ethyl cysteinate dimer in normal subjects and in patients with chronic cerebral infarction. *J Nucl Med* 1989;30:1018–1024.

33. Andersen AR. Technetium-99m-HMPAO: basic kinetic studies of a tracer of cerebral blood flow. *Cerebrovasc Brain Metab Rev* 1989;1:288–318.

34. Suess E, Huck S, Reither H, Hortnagl H, Angelberger P. Uptake mechanism of technetium-99m-d,1-HMPAO in cell cultures of the dissociated postnatal rat cerebellum. *J Nucl Med* 1992;33:108–114.

35. Moretti JL, Caglar M, Weinmann P. Cerebral perfusion imaging tracers for SPECT: which one to choose? *J Nucl Med* 1995;36:359–363.

Fluorine-18-FPH for PET Imaging of Nicotinic Acetylcholine Receptors

Andrew Horti, Ursula Scheffel, Marigo Stathis, Paige Finley, Hayden T. Ravert, Edythe D. London and Robert F. Dannals

Intramural Research Program, National Institute on Drug Abuse, Baltimore, Maryland; and Division of Nuclear Medicine, Department of Radiology, The Johns Hopkins Medical School, Baltimore, Maryland

Visualization of central nicotinic acetylcholine receptors (nAChRs) with modern PET or SPECT imaging techniques has been hampered by the lack of a radioligand with suitable in vivo binding characteristics (i.e., high target-to-nontarget ratios and kinetics appropriate for the half-life of the tracer and imaging modality used). This paper describes in vivo binding, kinetics and pharmacology of a highly potent ^{18}F-labeled analog of epibatidine, ($\pm$)-exo-2-(2-[^{18}F]fluoro-5-pyridyl)-7-azabicyclo[2.2.1]heptane ([^{18}F]FPH), in the mouse brain with the view towards application of this tracer for PET imaging of nAChR in human brain. **Methods:** Fluorine-18-FPH was administered intravenously to mice, and time-activity curves were determined for several regions in the brain and other organs. Saturation and pharmacology of [^{18}F]FPH binding was demonstrated in vivo by preinjecting unlabeled FPH or other drugs with known pharmacological action before [^{18}F]FPH was injected. The effect of the drugs on [^{18}F]FPH accumulation was evaluated. **Results:** [^{18}F]FPH was rapidly incorporated into the mouse brain; peak activity (2.4% of the injected dose) was measured at 5 min after intravenous administration, followed by washout to 1.1% injected dose (ID) at 60 min. Highest concentrations of ^{18}F occurred at 15 min in areas known to contain high densities of nAChR {e.g., thalamus [9.7% of injected dose per gram tissue (ID/g)] and superior colliculus (8.3% ID/g)}. Accumulation of the ^{18}F tracer in hippocampus, striatum, hypothalamus and cortical areas was intermediate (5.0, 5.6, 4.2 and 5.6% ID/g, respectively) and low in the cerebellum (2.8% ID/g). The distribution of [^{18}F]FPH in the mouse brain matched that of other in vivo nAChR probes such as ^{3}H-labeled epibatidine or norchloroepibatidine, [^{3}H](−)-nicotine and [^{3}H]cytisine and that of nAChR densities determined in postmortem autoradiographic studies in rodents. Preinjection of blocking doses of unlabeled epibatidine, (−)-nicotine, lobeline and cytisine significantly inhibited [^{18}F]FPH binding in thalamus and superior colliculus, but not in cerebellum, whereas drugs that interact with binding sites other than acetylcholine recognition sites of nAChR (e.g., mecamylamine, scopolamine, N-methylspiperone and ketanserin) had no effect on [^{18}F]FPH accumulation in any of the brain regions examined. **Conclusion:** Fluorine-18-FPH labels nAChR in vivo in the mouse brain. Because of its high uptake into the brain and high ratios of specific-to-nonspecific binding, this radioligand appears to be ideally suited for PET imaging of nAChR in the mammalian brain.

Key Words: nicotinic acetylcholine receptor; brain imaging; PET

J Nucl Med 1997; 38:1260–1265

Cerebral nicotinic acetylcholine receptors (nAChRs), important sites of excitatory neurotransmission in brain, have been

studied extensively. Molecular biological techniques have been applied in determining the amino acid sequences of the subunits that compose the receptor (1–3), autoradiographic techniques have been used to delineate the anatomical distribution of nAChRs in brain (4–7) and metabolic mapping studies have demonstrated that the specific binding sites labeled in brain with specific radioligands are coupled to functional activity (8). Human investigations have provided evidence for a critical role of nAChRs in cognition and in the pathogenesis of Alzheimer's (9) and Parkinson's diseases (10). Furthermore, nAChRs are the sites of action of nicotine, the ingredient that promotes tobacco addiction, a disorder to which over 400,000 deaths a year are attributed in the U.S. (11).

Despite the critical function of nAChRs in normal physiology and in disorders of brain function, a suitable probe for assaying this receptor noninvasively in the human brain is not available. (−)-S-[^{11}CH$_3$]Nicotine has been used to image nAChRs in monkey (12,13) and human (14) brain using PET. Studies of patients with Alzheimer's disease showed less uptake of both (+)-(R)- and (−)-S-[^{11}CH$_3$]nicotine in the brain as compared with uptake in age-matched controls, consistent with the profound loss of nAChRs in postmortem material from patients who died with the disease (15,16). Nonetheless, rapid egress of radiolabeled nicotine from the brain and high levels of nonspecific binding (7,14) limit the utility of isotopically labeled nicotine as a tracer for PET. Another nicotinic agonist, [^{3}H]cytisine, has been evaluated for the purpose of in vivo labeling of nAChRs in mouse brain (17). Although this ligand has a slower clearance from brain than does [^{3}H]nicotine, and considerably less nonspecific binding, relatively poor penetration of the blood-brain barrier suggested that labeling cytisine for PET studies would not be worthwhile.

Impetus for further work on development of radioligand probes for in vivo labeling of nAChRs has been provided by the discovery of epibatidine, an alkaloid extracted from the skin of the Ecuadorian poisonous frog *Epipedobatus tricolor* (18) and its characterization as (+)-exo-2-(2-chloro-5-pyridyl)-7-azabicyclo[2.2.1]heptane (19,20). Studies in mice demonstrated that peripherally administered epibatidine was an extremely potent antinociceptive agent, suggesting a central action (21), and its structural similarity to nicotine suggested that the alkaloid might have activity at nAChRs (22). Indeed, the latter hypothesis was confirmed in receptor binding assays indicating that epibatidine inhibited the binding of [^{3}H]nicotine and [^{3}H]cytisine but not that of radioligands selective for a variety of other neurotransmitter receptors (21,23–25). Both enantiomeric forms of epibatidine, the natural (+)- and the

synthetic (−)-isomer, displayed similar binding activity in vivo (21). In vitro functional assays demonstrated that epibatidine was a potent agonist at neural and neuromuscular nAChRs (25) and more potent than nicotine in enhancing ^{86}Rb flux in IMR 32 cells and in increasing [3H]dopamine release from rat striatal slices (26). Additional behavioral studies indicated that the antinociceptive action of epibatidine was blocked by the centrally acting nAChR antagonist mecamylamine and that the drug was more potent than nicotine in reducing locomotor activity and body temperature in mice (26,27). In rats trained with nicotine, epibatidine engendered nicotine-like responding that was blocked by mecamylamine but not by hexamethonium, a peripheral antagonist (27). When a radiolabeled form of epibatidine became available, in vitro binding assays with [3H]epibatidine demonstrated that the ligand bound to two populations of sites in rat and human brain, with extremely high affinities (K_d values = 12 pM, 200 pM in rat brain; <1 pM in human brain) (28). Subsequent in vivo studies of biodistribution and pharmacological specificity of [3H]epibatidine in the mouse identified this tracer as the most promising in vivo radioligand for nAChRs ever studied and suggested that analogs of epibatidine, labeled appropriately for PET or SPECT imaging, might be useful probes for human investigation (29). Similar studies as with [3H]epibatidine were performed with the (+) and (−) isomers of [3H]norchloroepibatidine and demonstrated selective binding to nAChR in the rodent brain, high ratios of specific to nonspecific binding and appropriate in vivo kinetics, all necessary attributes for a successful receptor ligand for imaging purposes (30). The promising findings on the in vivo binding of [3H]epibatidine and norchloro analogs prompted this investigation.

The purpose of this study was to assess the utility of (±)-exo-2-(2-[18F]fluoro-5-pyridyl)-7-azabicyclo[2.2.1]heptane ([18F]FPH) (31), a labeled analog of epibatidine, for development as a radiotracer to study nAChRs in brain-using PET. The radioligand was tested in in vivo assays of biodistribution and pharmacological specificity in the mouse brain.

MATERIALS AND METHODS

Ligands

No-carrier-added [18F]FPH (Fig. 1) and authentic (±)-exo-2-(2-fluoro-5-pyridyl)-7-azabicyclo[2.2.1]heptane (FPH) were prepared as previously described (31). Briefly, a solution of (±)-exo-2-(2-bromo-5-pyridyl)-7-azabicyclo[2.2.1]heptane in dimethyl sulfoxide was heated with K[18F]/Kryptofix 222® complex for 15 min at 200°C. The labeled product was purified by preparative high performance liquid chromatography. Chemical and radiochemical purities determined by high performance liquid chromatography (HPLC) exceeded 95%. Sterility and apyrogenicity testing were performed using standard procedures. The average specific activity of the final product calculated at the end of synthesis was greater than 2000 mCi/μmol. The specific activity was determined as previously described (31). Authentic, unlabeled FPH, used as a standard in HPLC, was prepared by Kryptofix 222®-assisted nucleophilic fluorination of (±)-exo-2-(2-bromo-5-pyridyl)-7-methoxy carbonyl-7-azabicyclo[2.2.1]heptane followed by acid deprotection.

Drugs

(±)-Epibatidine dihydrochloride, (+)-epibatidine L-tartrate, (−)-nicotine bitartrate and mecamylamine hydrochloride were purchased from Research Biochemical International, Natick, MA. Cytisine and apomorphine hydrochloride were obtained from Sigma Chemical Co., St. Louis, MO. The drugs were dissolved shortly before each experiment. (±)- and (+)-epibatidine salts

were stored in acetonitrile and ethanol, respectively. Shortly before use in animals, the solvent was evaporated under nitrogen, and the residue dissolved in saline.

Animal Studies

All experimental protocols were approved by the Animal Care and Use Committee of the Johns Hopkins Medical Institutions. Male CD1 mice weighing 23–33 g were used in all experiments. For kinetic studies, each mouse received 200 μCi of [18F]FPH (specific activity = 2000–4000 mCi/μmol), dissolved in 0.2 ml saline by injection into a tail vein. At different times after tracer administration the animals were killed by cervical dislocation, and the brains were quickly removed and dissected on ice as previously described (32), weighed and assayed for regional radioactivity as outlined below.

In vivo receptor blocking studies were performed by administering subcutaneous injections of selected drugs of known pharmacological action to mice, followed by intravenous (i.v.) injection of the [18F]FPH tracer (20–200 μCi). Both the drug and the tracer were dissolved in 0.9% NaCl and administered in a volume of 0.2 ml. Thirty minutes after administration of the tracer, brain tissues were harvested, weighed, placed in plastic tubes and then radioactivity assayed in an automatic gamma counter. The counting error was kept below 3%. Aliquots of the injectate were prepared as standards and counted along with the tissue samples. The percent injected dose per gram of tissue (%ID/g) and the percent injected dose per organ (%ID/organ) were calculated.

For assay of the whole body distribution and the estimation of radiation doses to individual organs, mice (n = 3 for each time point) received 20 μCi [18F]FPH i.v. and were killed at different times after injection. A 0.1-ml blood sample was obtained, and organs (brain, lungs, heart, liver, spleen, kidneys, testes, stomach, upper and lower gastrointestinal), as well as samples of muscle and bone, were removed, weighed, and assayed for radioactivity. In the bladder, complete collection of urine was assured by ligation of the external urethral meatus (under short ether anesthesia) before the tracer was injected.

Determination of Metabolites

For analysis of metabolites, a urine sample (0.8 ml, 23 μCi) was collected over 60 min after injection and was adjusted to pH 8.5 with a concentrated solution of $NaHCO_3$ and extracted with methylene chloride. The organic layer was evaporated under vacuum, and the residue (16 μCi) was redissolved in HPLC mobile phase (H_2O/CH_3CN/trifluoroacetic acid, 12.5:87.5:0.15) and injected onto a HPLC column (Alltech Econosil C18, 4.6 × 250 mm; flow rate: 3 ml/min). Under these conditions, the [18F]FPH and a labeled metabolite were eluted with retention times of 4.9 min and 2.9 min, respectively. HPLC analysis was performed with a HPLC pump (Waters 590EF), an in-line fixed wavelength (254 nm) detector and a single 2-inch NaI crystal radioactivity detector. The HPLC chromatograms were recorded by a Rainin Dynamax dual channel control/interface module connected to a Macintosh computer with appropriate software (Dynamax, version 1.3).

Statistical Analysis

Data were analyzed by ANOVA with Dunnett's posthoc test for comparing treatment means to control values. Differences were considered significant at p < 0.05.

RESULTS

Fluorine-18-FPH was rapidly incorporated into the mouse brain, with 2.36 ± 0.13% (mean of 3; ± s.e.m.) of the injected dose present in the whole brain at 5 min after injection and washout to 1.10% of the dose at 60 min. Time-activity curves of [18F]FPH in cerebellum, hippocampus, superior colliculus and thalamus are shown in Figure 2. The highest accumulation of
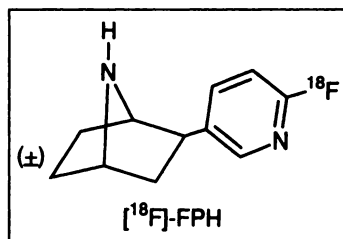
FIGURE 1. Structure of (±)-exo-(2-[¹⁸F]fluoro-5-pyridyl)-7-azabicyclo[2.2.1]heptane ([¹⁸F]FPH).

¹⁸F occurred in thalamus and superior colliculus, intermediate radioactivity was found in the hippocampus and lowest radioactivity in the cerebellum. The initial clearance rate (i.e., that between 5 and 60 min postinjection) of [¹⁸F]FPH from the cerebellum was higher than from any other region studied, presumably because the cerebellum is an area with relatively few nAChRs (7,17,33). By contrast, in regions with high densities of nAChRs (e.g., the thalamus and superior colliculus), tissue-to-cerebellar ratios increased steadily over the observation period, reaching values of 15.0 and 11.4, respectively, 3 hr after injection (Fig. 3).

The pharmacology of [¹⁸F]FPH in vivo binding to nAChRs was studied under several conditions. Subcutaneous preinjection of different doses of unlabeled epibatidine 30 min before injection of the tracer resulted in a dose-dependent inhibition of [¹⁸F]FPH binding in all regions of the mouse brain examined, except in the cerebellum (Fig. 4).

Similarly, preinjection of increasing doses of the nAChR agonist (−)-nicotine resulted in dose-dependent blocking of [¹⁸F]FPH binding. Figure 5 shows the significant, dose-dependent decreases in [¹⁸F]FPH accumulation observed in the nAChR-rich thalamus and superior colliculus after preadministration of (−)-nicotine. Less inhibition of [¹⁸F]FPH accumulation was seen in the hippocampus, and no observable effect occurred in the cerebellum. Using the values of percent of injected dose (Fig. 5) and considering cerebellar concentrations of the tracer as estimates for nonspecific binding (34), ED$_{50}$ values for the inhibition of [¹⁸F]FPH binding in the thalamus and superior colliculus were calculated to be 2.2 and 2.1 μmol of (−)-nicotine/kg body weight, respectively.

Other nicotinic receptor ligands, such as cytisine and lobeline, inhibited [¹⁸F]FPH binding as well (Fig. 6). By contrast, mecamylamine, a noncompetitive nAChRs antagonist, scopolamine, a muscarinic cholinergic antagonist and noncholinergic drugs, such as apomorphine (dopamine receptor agonist) and N-methylspiperone (a D2-dopamine receptor antagonist) or ketanserin (a 5-HT$_2$/5-HT$_{1C}$ serotonin receptor antagonist) were without effect.

As a step preliminary to using [¹⁸F]FPH in human studies and evaluating radiation dose estimates, the whole-body biodistribution of [¹⁸F]FPH was determined at different times after administration. [¹⁸F]FPH was injected i.v. into mice, and the time-dependent distribution in selected organs was assayed (Fig. 7). [¹⁸F]FPH was rapidly eliminated from the body via urinary excretion with up to 60% of the injected dose appearing in the bladder at 4 hr. Relatively high initial (15 min after injection) accumulation of [¹⁸F]FPH occurred in the muscle from which the tracer was subsequently cleared very rapidly. Uptake of ¹⁸F in the total bone was low (<1.2% of the injected dose). Radiation absorbed dose estimates revealed the bladder as the critical organ. Detailed information on radiation doses to individual organs calculated by the absorbed dose method (35) are available from the authors on request.

DISCUSSION

The most important findings from this study are summarized as follows:

1. The distribution of the new ¹⁸F-labeled epibatidine analog [¹⁸F]FPH is comparable to that of [³H]epibatidine (29) and of ³H-labeled isomers of norchloroepibatidine (30).
2. It parallels that of other in vivo labels of nAChR (e.g., [³H]cytisine and [³H]-(−)nicotine (17,33).
3. The pharmacology of [¹⁸F]FPH in vivo confirms selective binding to nAChR and no binding to other receptors, such as serotonergic, D2-like dopaminergic and muscarinic acetylcholine receptors.
4. Whole-body distribution studies show elimination of the tracer primarily though urinary excretion, and radiation dose estimates determine the bladder to be the critical organ (1.12 rads/mCi injected dose over the first 4 hr after injection).

Fluorine-18-FPH showed rapid uptake into the whole mouse brain Fluorine-18- with peak uptake (2.4% of the injected dose) occurring at 5 min after i.v. administration. Thereafter, the ¹⁸F radioactivity declined gradually over the next 55 min. This pattern of kinetics in the whole brain by [¹⁸F]FPH contrasted with that of [³H]epibatidine and [³H]norchloroepibatidine, tracers which enter the brain more slowly and show peak uptake as late as 30 min after injection (29,30).

The regional distribution of [¹⁸F]FPH in the mouse brain was similar to that of [³H]epibatidine (29) and [³H]-labeled isomers of norchloroepibatidine (30) and paralleled the distribution of nicotinic acetylcholine receptors in the brain as determined in vivo using other radioligands for nAChR (7,17,33). Of all brain regions examined, maximal concentrations of [¹⁸F]FPH were observed in the thalamus (9.7% ID/g tissue) and superior colliculus (8.2% ID/g) 15 min after i.v. administration (as shown in Fig. 1). These peak radioactivity concentrations were considerably lower than those previously observed with [³H]epibatidine (27.6 and 23.5% ID/g in thalamus and superior colliculus, respectively, at 60 min after injection) (29). However, when specific binding, expressed as the ratio thalamus/cerebellum, was considered, [¹⁸F]FPH was comparable to [³H]epibatidine, reaching a ratio of 15 at 3 hr versus 13 for the tritiated analog at 4 hr.

Given the relatively high ratios between [¹⁸F]FPH binding in nAChR-rich (thalamus) and nAChR-poor (cerebellum) regions of the mouse brain, excellent visualization of the distribution of central nAChR, as well as good resolution in PET images are to be expected using this tracer.

The regional distribution of [¹⁸F]FPH in the mouse brain correlated well not only with that of [³H]epibatidine (r = 0.90) but also with that of [³H]cytisine (r = 0.92), another ligand with high affinity towards nAChR (17). The superposition of [¹⁸F]FPH and [³H]cytisine binding sites point to the possibility that both tracers label the same subtypes of nAChRs in vivo in the mouse brain. Indeed, previous studies using in vitro binding assay techniques as well as functional assays found that in the rodent brain both (±) epibatidine and (−)-cytisine are bound to the same subtypes of nicotinic receptors, i.e., to α4β2 and, to a lesser extent, to α3βx (36).

Pharmacological studies, performed by preinjecting drugs with known binding sites, confirmed the selective binding of [¹⁸F]FPH to nicotinic receptors in the mouse brain. Blocking of [¹⁸F]FPH binding sites with nAChRs agonists, (−)-nicotine, (±)-epibatidine, cytisine and lobeline, revealed competitive, dose-dependent effects of these drugs. The blocking effect of these agonists appeared to be more pronounced in high density
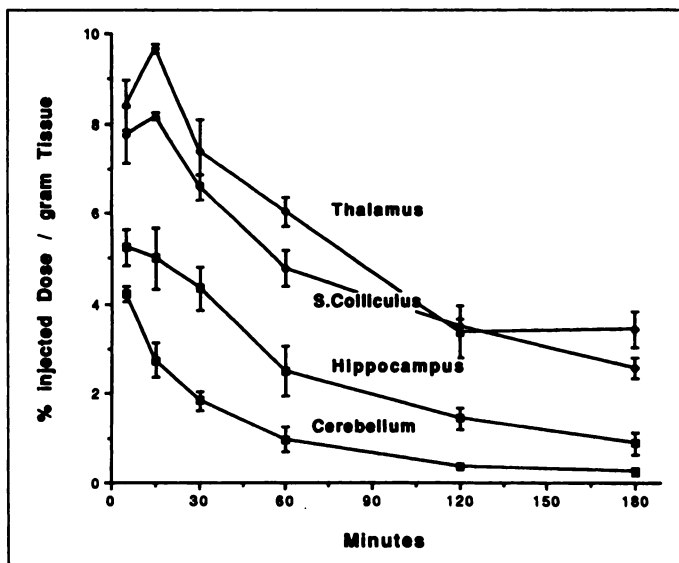
FIGURE 2. Kinetics of [18F]FPH in cerebellum, hippocampus, superior colliculus and thalamus of the mouse brain. Mice (n = 3 for each time point) received 200 μCi of [18F]FPH intravenously. At different times after injection, the animals were killed and radioactivity concentrations determined in different brain regions. Data are means ± s.e.m.

FIGURE 3. Tissue-to-cerebellar ratios of [18F]FPH concentrations at different times after i.v. injection into mice. Data and presentation are the same as in Figure 2.

areas (thalamus, superior colliculus) than in intermediate density regions (striatum, hippocampus and cortical areas) and very little in the cerebellum (see Figs. 4 and 5). On the other hand, mecamylamine, a nicotinic acetylcholine receptor channel blocker and scopolamine, a drug that is active at the muscarinic acetylcholine receptor, had no influence on [18F]FPH binding to nAChR.

Whole-body time-uptake curves (Fig. 7) in different areas of the mouse body demonstrated high (25% ID) initial uptake in the muscle mass, with 95% clearance within 120 min after injection. Whether or not this finding represents temporary binding of [18F]FPH to nAChR at the neuromuscular junction, e.g., to the $\alpha 1$, $\beta 1$, δ, γ subtype of nAChR, remains to be determined. Accumulation of [18F]FPH in liver and kidneys, on the other hand, amounted to only 9% and 4% ID, respectively. Fluorine-18-FPH was rapidly eliminated from the body through the bladder. To determine the composition of the excreted
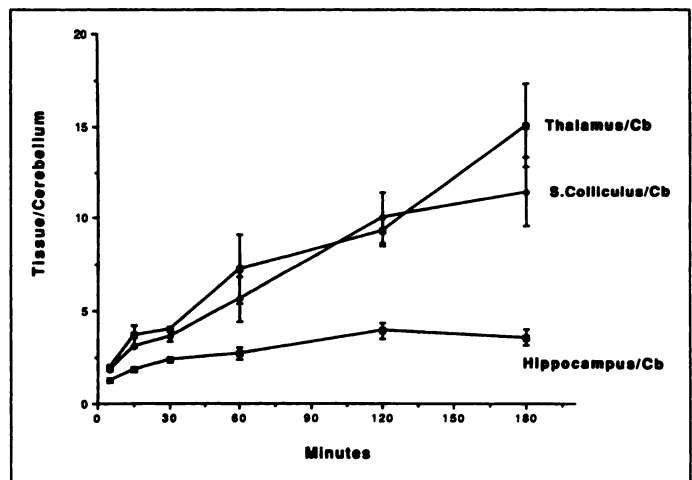
radioactivity, mouse urine, obtained 60 min after injection, underwent preliminary metabolite analysis by reverse phase HPLC. About 70% of the extracted radioactivity was found to be unchanged [18F]FPH, whereas 30% of the radioactivity was attributable to a more hydrophilic compound with shorter retention time. The nature of this [18F]-labeled metabolite has not been identified at this time.

Uptake of radiolabeled fluoride ($^{18}F^-$) in the total bone after injection of [18F]FPH was low (1.2% ID at 15 min post-injection) and decreased to 0.45% ID at 4 hr. This may be due to the rapid elimination of the radioligand via the urinary tract, as well as little or no metabolism of the tracer to $^{18}F^-$. Since 2-fluoropyridine derivatives have been shown to undergo hydrolytic decomposition (37), some decomposition of [18F]FPH with formation of $^{18}F^-$ in vivo was to be expected; however, no significant decomposition of [18F]FPH by hydrolysis of the C-^{18}F bond occurred in vivo during the 4 hr time of observation.

Since epibatidine and its analogs are highly toxic, utmost care has to be taken in the preparation of the tracer for i.v. injection. In mice, given injections of up to 200 μCi [18F]FPH (0.1 nmol/mouse or 4 nmol/kg, or 0.8 μg/kg), no untoward pharma-
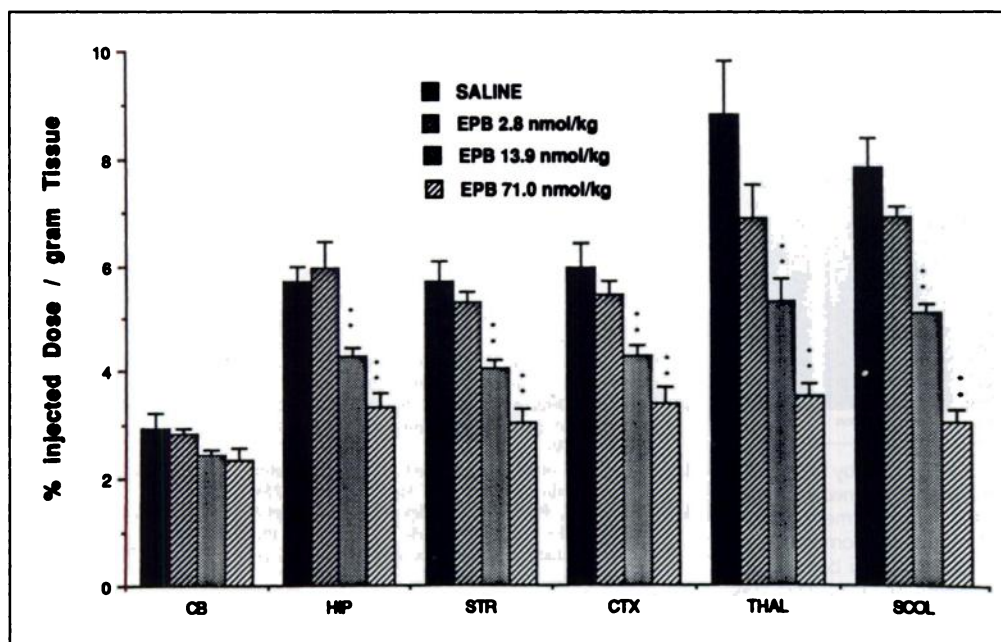

FIGURE 4. Unlabeled epibatidine decreases [18F]FPH binding in a dose-dependent manner in all central nervous system regions examined, except in the cerebellum. (±)Epibatidine dihydrochloride at the 1 and 5 μg/kg levels (2.8 and 14 nmol/kg, respectively) and (+)epibatidine tartrate at the 20 μg/kg dose level (71 nmol/kg) were injected s.c. 30 min before tracer administration. The animals were killed 30 min after i.v. injection of [18F]FPH. CB = cerebellum; HIP = hippocampus; STR = striatum; CTX = cortex; THAL = thalamus; SCOL = superior colliculus. Data are means ± s.e.m. (n = 3)

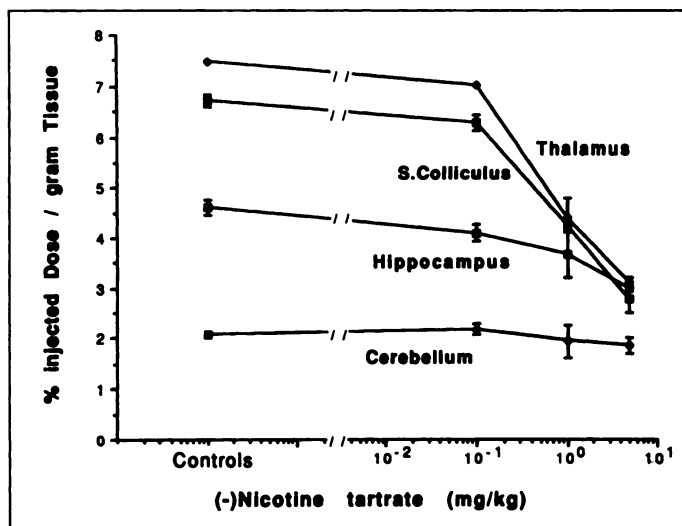**FIGURE 5.** Dose-dependent inhibition of [^{18}F]FPH binding by (−)nicotine bitartrate, injected s.c. 5 min before i.v. tracer administration. The mice (n = 3) were killed 30 min after [^{18}F]FPH injection. Data are means ± s.e.m.

cological effects were noticed after administration of the tracer. However, higher i.v. doses of unlabeled FPH (>5 μg/kg) caused cardiorespiratory effects and severe seizures and were followed by death in the majority of the animals consistent with the reported pharmacological effects of epibatidine (*38*). Besides being a potent agonist of central nAChRs, epibatidine is also a powerful ganglionic depolarizing agent (*38*). To prevent these detrimental effects of the drug, it is therefore mandatory that [^{18}F]FPH be administered in high specific activity (>2000 mCi/μmol). From preliminary data obtained by imaging nAChR in baboon brain (*39*), it is anticipated that a dose of 5 mCi of high specific activity [^{18}F]FPH will be sufficient for PET studies in humans.

CONCLUSION

The newly synthesized radiotracer [^{18}F]FPH labels nicotinic acetylcholine receptors in the central nervous system of mice, after i.v. administration. Rapid association of the tracer to nAChRs in receptor-rich areas and rapid egress from receptor-poor areas led to high ratios of specific-to-nonspecific binding. [^{18}F]FPH and PET should prove useful for the localization and quantitation of nicotinic AChRs in normal physiological and pathological states.
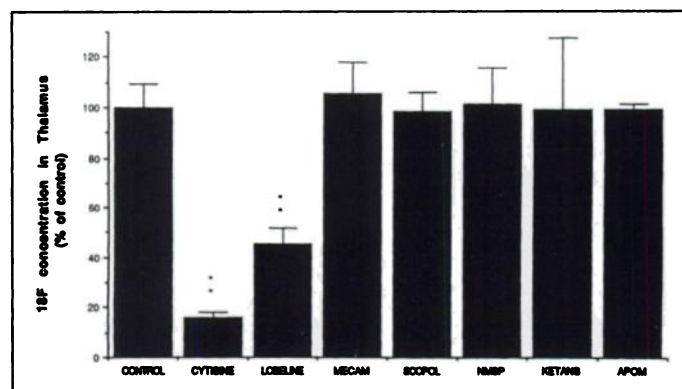

FIGURE 6. Inhibition of [^{18}F]FPH binding in mouse thalamus by preinjection of cytisine (5.0 mg/kg) and lobeline (20 mg/kg), but not by mecamylamine (MECAM; 5.0 mg/kg), scopolamine (SCOPOL; 10.0 mg/kg), N-methyl-spiperone (NMSP; 1.0 mg/kg), ketanserin (KETANS; 1 mg/kg) or apomorphine (10 mg/kg). All drugs were administered subcutaneously 30 min before tracer injection except lobeline, which was given 2 min before. The mice were killed either 30 min (mice that had received MECAM or SCOPOL) or 60 min after i.v. injection of [^{18}F]FPH. Data are means ± s.e.m. (n = 3). * p < 0.05; ** p < 0.01
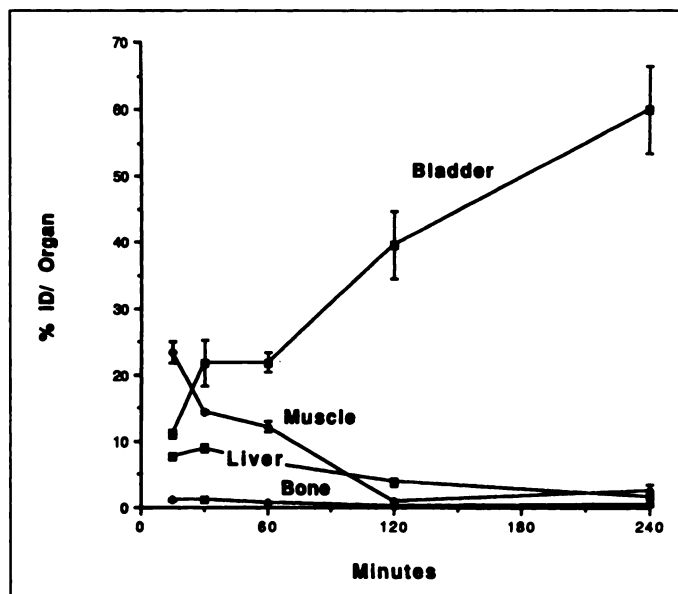

FIGURE 7. [^{18}F] concentrations in urine (bladder), liver, kidneys, bone and muscle at different times after i.v. injection of [^{18}F]FPH into mice. Data are means ± s.e.m. (n = 3). Total muscle was assumed to be 40% of the body weight; total bone was calculated by multiplying the radioactivity in one femur by 5.

NOTE ADDED IN PROOF

While this article was in review, a study by Ding et al. (*40*) was published showing similar data on in vivo binding of [^{18}F]FPH (NFEP) to nAChRs.

ACKNOWLEDGMENTS

REFERENCES

1. Deneris E, Bouler J, Connolly J, et al. Genes encoding neuronal nicotinic acetylcholine receptors. *Clin Chem* 1989;35:731–737.
2. Cheney DL. Neuronal nAChRs: molecular biology. *Neurosci Facts* 1991;2:2–3.
3. McKay J, Lindstrom J, Loring RH. Determination of nicotinic receptor subtypes in chick retina using monoclonal antibodies and ^{3}H-epibatidine. *Med Chem Res* 1994;4: 528–537.
4. Boksa P, Quirion R. [^{3}H]N-methylcarbamylcholine: a new radioligand specific for nicotinic acetylcholine receptors in brain. *Eur J Pharmacol* 1987;139:323–333.
5. London ED, Waller SB, Wamsley JK. Autoradiographic localization of [^{3}H]nicotine binding sites in the rat brain. *Neurosci Lett* 1985;53:179–184.
6. Perry DC, Kellar KJ. [^{3}H]epibatidine labels nicotinic receptors in rat brain: autoradiographic study. *J Pharmacol Exp Ther* 1995;285:1030–1034.
7. Broussolle EP, Wong DF, Fanelli RJ, London ED. In vivo specific binding of [^{3}H]l-nicotine in the mouse brain. *Life Sci* 1989;44:1123–1132.
8. London ED, Connolly RJ, Szikszay M, Wamsley JK, Dam M. Effects of nicotine on local cerebral glucose utilization in the rat. *J Neurosci* 1988;8:3920–3928.
9. Schroder H, Giacobini E, Wevers A, Birtsch C, Schutz U. Nicotinic receptors in Alzheimer's disease. In: *Brain Imaging of nicotine and tobacco smoking.* Ann Arbor, MI, NPP Books; 1995:73–93.
10. Court JA, Perry EK. CNS nicotinic receptors: possible therapeutic targets in neurodegenerative disorders. *CNS Drugs* 1994;2:216–233.
11. Centers for Disease Control and Prevention. Cigarette smoking—attributable mortality and years of potential life lost—United States, 1988. *Morb Mortal Wkly Rep* 1993;42:37–39.
12. Maziere M, Comar D, Marazano C, Berger G. Nicotine-^{11}C: synthesis and distribution kinetics in animals. *Eur J Nucl Med* 1976;1:255–258.
13. Nordberg A, Hartvig P, Lundqvist H, et al. Uptake and regional distribution of (+)-(R)- and (−)-(S)-(N-methyl-^{11}C)-nicotine in the brains of Rhesus monkeys: an attempt to study nicotinic receptors in vivo. *J. Neural Transm Parkinson's Dis Dementia Sect* 1989;1:195–205.
14. Nyback H, Nordberg A, Långström B, et al. Attempts to visualize nicotinic receptors in the brain of monkey and man by positron emission tomography. *Prog Brain Res* 1989;79:313–319.

15. Whitehouse PJ, Martino AM, Antuono PG, et al. Nicotinic acetylcholine binding sites in Alzheimer's disease. *Brain Res* 1986;371:146–151.
16. London ED, Ball MJ, Waller SB. Nicotinic binding sites in cerebral cortex and hippocampus in Alzheimer's dementia. *Neurochem Res* 1989;14:745–750.
17. Flesher JE, Scheffel U, London ED, Frost JJ. In vivo labeling of nicotinic cholinergic receptors in brain with [³H]cytisine. *Life Sci* 1994;54:1883–1890.
18. Daly JW, Brown GB, Mensah-Dwumah M, Myers CW. A new class of indolizidine alkaloids from the poison frog, *Dendrobates tricolor*: x-ray analysis of 8-hydroxy-8-methyl-6-(2'-methylhexylidene)-1-azabicyclo[4.3.0]nonane. *J Am Chem Soc* 1980; 102:830–836.
19. Daly JW, Myers CW, Whittaker N. Further classification of skin alkaloids from neotropical poison frogs (dendobatidae), with a general survey of toxic/noxious substances in the amphibia. *Toxicon* 1987;25:1023–1095.
20. Spande TF, Garaffo HM, Edwards MW, Yeh HJC, Pannell L, Daly JW. Epibatidine: a novel (chloropyridyl)azabicycloheptane with potent analgesic activity from an Ecuadorian poison frog. *J Am Chem Soc* 1992;114:3475–3478.
21. Badio B, Daly JW. Epibatidine, a potent analgetic and nicotinic agonist. *Mol Pharmacol* 1994;45:563–569.
22. Badio B, Garraffo HM, Spande TF, Daly JW. Epibatidine: discovery and definition as a potent analgesic and nicotinic agonist. *Med Chem Res* 1994;4:440–448.
23. Qian C, Li T, Shen TY, Libertine-Garahan L, Eckman J, Biftu T, Ip S. Epibatidine is a nicotinic analgesic. *Eur J Pharmacol* 1993;250:R13–R14.
24. Dukat M, Damaj MI, Glassco W, et al. Epibatidine: a very high affinity nicotine-receptor ligand. *Med Chem Res* 1993;4:131–139.
25. Bonhaus DW, Bley KR, Broka CA, et al. Characterization of the electrophysiological, biochemical and behavioral actions of epibatidine. *J Pharmacol Exp Ther* 1995;272: 1199–1203.
26. Sullivan JP, Decker MW, Brioni JD, et al. (±)-Epibatidine elicits a diversity of in vitro and in vivo effects mediated by nicotinic acetylcholine receptors. *J Pharmacol Exp Ther* 1994;271:624–631.
27. Damaj MI, Creasy KR, Grove AD, Rosecrans JA, Martin BR. Pharmacological effects of epibatidine optical enantiomers. *Brain Res* 1994;664:34–40.
28. Houghtling RA, Davila-Garcia MI, Kellar KJ. Characterization of (+)-[³H]epibatidine binding to nicotinic cholinergic receptors in rat and human brain. *Mol Pharmacol* 1995;48:280–287.
29. London ED, Scheffel U, Kimes AS, Kellar KJ. In vivo labeling of nicotinic acetylcholine receptors in brain with [³H]epibatidine. *Eur J Pharmacol* 1995;278:R1–R2.
30. Scheffel U, Taylor GF, Kepler JA, Carroll FI, Kuhar MJ. In vivo labeling of neuronal nicotinic acetylcholine receptors with radiolabeled isomers of norchloroepibatidine. *NeuroReport* 1995;6:2483–2488.
31. Horti AG, Ravert HT, London ED, Dannals RF. Synthesis of a radiotracer for studying nicotinic acetylcholine receptors by positron emission tomography: (±)-exo-2-(2-[¹⁸F]fluoro-5-pyridyl)-7-azabicyclo[2.2.1]heptane. *J Lab Compd Radiopharm* 1996; 38:355–366.
32. Scheffel U, Ricaurte GA. Paroxetine as an in vivo indicator of 3,4-methyl-enedioxymethamphetamine neurotoxicity: a presynaptic serotonergic positron emission tomography ligand? *Brain Res* 1990;527:89–95.
33. London ED, Waller SB, Wamsley JK. Autoradiographic localization of [³H]nicotine binding sites in the rat brain. *Neurosci Lett* 1985;53:179–184.
34. Scheffel U, Pögün S, Stathis M, Boja JW, Kuhar MJ. In vivo labeling of cocaine binding sites on dopamine transporters with [³H]WIN 35,428. *J Pharmacol Exp Ther* 1991;257:954–958.
35. Snyder WS, Ford MR, Warner GG, Watson SB. "S," absorbed dose per unit cumulated activity for selected radionuclides and organs. In: *NM/MIRD Pamphlet No.11*. Oak Ridge, TN: Oak Ridge National Laboratory; 1975.
36. Decker MW, Brioni JD, Bannon AW, Americ SP. Diversity of neuronal nicotinic acetylcholine receptors: lessons from behavior and implications for CNS therapeutics. *Life Sci* 1995;56:545–570.
37. Bradlow HL, Vanderwerf CA. Studies on the acid hydrolysis of α-halogenated pyridine compounds. *J Org Chem* 1949;14:509–515.
38. Fisher M, Huangfu D, Shen TY, Guyenet PG. Epibatidine, an alkaloid from the poison frog Epipedobates tricolor, is a powerful ganglionic depolarizing agent. *J Pharmacol Exp Ther* 1994;270:702–707.
39. Villemagne VL, Horti A, Scheffel U, Ravert HT, Finley P, London ED, Dannals RF. Imaging nicotinic acetylcholine receptors in baboon brain by PET [Abstract]. *J Nucl Med* 1996;37(suppl):37:11P.
40. Ding Y-S, Gatley J, Fowler JS, et al. Mapping nicotinic acetylcholine receptors with PET. *Synapse* 1996;24:403–407.